The Cryosphere Discuss., doi:10.5194/tc-2016-138, 2016
Manuscript under review for journal The Cryosphere
Published: 18 July 2016

Characteristics of an avalanche-feeding and partially debris-covered glacier and its response to atmospheric warming in Mt. Tomor, Tian Shan, China

Puyu Wang[1], Zhongqin Li[1,2], Huilin Li[1]

[1]State Key Laboratory of Cryosphere Science/Tianshan Glaciological Station, Cold and Arid Regions Environmental and Engineering Research Institute, Chinese Academy of Sciences, Lanzhou, 730000, China;

[2]College of Geography and Environment Science, Northwest Normal University, Lanzhou, 730070, China

Correspondence to: Puyu Wang (wangpuyu@lzb.ac.cn)

Abstract. Qingbingtan Glacier No. 72 in Mt. Tomor region is a small cirque-valley glacier with complex topography and debris-covered areas. Investigating its variation process will provide meaningful information for understanding the response of debris-covered glaciers existing broadly to climate change. The glacier accumulation area is characterized by receiving large amounts of precipitation and experiencing frequent snow/ice avalanches; temperature and flow regimes are analogous to a temperate or a monsoonal maritime glacier. Data from in-situ observations since 2008 and digitized earlier maps indicate the glacier has been in retreat and experienced thinning during the past 50 years. Between 1964 and 2008, its terminus retreat was 41 m a^{-1}, area reduction was 0.034 km^2 a^{-1}, and its thickness decreased at an average rate of 0.6 m a^{-1} in the ablation area. With the melting enhancing, the proportion of the debris-covered area and thickness increased as well as inhibition of debris cover to melting. Thus, despite the persistent atmospheric warming during the last several decades, the strongest ablation and most significant terminus retreat and area reduction of the glacier occurred at the end of the last century and the beginning of this century rather than in most recent years. Based on a

comprehensive analysis of climate change, glacier response delay, glacial topographic features and debris-cover influence, the glacier will continue to retreat in the upcoming decades, yet with a gradually decreasing speed. Then it will stabilize after its terminus retreats to an elevation of approximately 4000 m a.s.l.

Keywords: Glacier recession; debris cover; Mt. Tomor; Tian Shan; atmospheric warming

1. Introduction

In the past decades, atmospheric warming has caused the majority of the glaciers to recede on a global scale, with the acceleration of the recession remarkably (Haeberli et al., 2002; Oerlemans, 2005; Meier et al., 2007; Arendt et al., 2012; Yao et al., 2012; IPCC, 2013; Farinotti et al., 2015; Zemp et al., 2015). Because glacial recession plays essential roles in affecting sea level, water resources and the environment, glacier variation has become the attention focus of not only scientific communities, but of the all publics (Raper and Braithwaite, 2006; Kehrwald et al., 2008; Berthier et al., 2010; Bliss et al., 2014). However, glacier variation is affected by multiple factors. Beside climatic conditions, morphology and glacier physical properties have also important influence on glacier variation, so that differences in glacier variation arise between various regions and even between different glaciers in a same region (Kutuzov and Shahgedanova, 2009; Narama et al., 2010). Therefore, although a number of studies have addressed glacial variation, at either global (Haeberli et al., 2000; Marzeion et al., 2012; Bliss et al., 2014) or regional scales (Bolch et al., 2011; Huss, 2012; Neckel et al., 2014; Fischer et al., 2014), or with local monitoring of glacial variation (WGMS, 2008a, 2008b, 2012, 2013; Li et al., 2010; Wang et al., 2011, 2013), it is still necessary to investigate the variation of different types of glaciers in different regions.

The Cryosphere Discuss., doi:10.5194/tc-2016-138, 2016
Manuscript under review for journal The Cryosphere
Published: 18 July 2016

There are a number of glaciers in the Tian Shan of China, Central Asia that inevitably and significantly influence local water resources, the environment and social economics. Generally, previous studies of the glaciers in the Tian Shan have revealed that, the glaciers have been in persistent recession during the last several decades, similar to the trends for most glaciers in other regions (Li et al., 2010; Wang S et al., 2011; Farinotti et al., 2015). However, few studies have documented the monitoring of typical glaciers of different types. Mt. Tomor, the highest peak of the Tian Shan (elevation 7439 m; Kyrgyz name: Jengish Chokosu; Russian name: Pik Pobedy), nourishes the largest glaciated region in the Tian Shan; glacial meltwater is the major water source for the Tarim Basin (Chen et al., 2008; Pieczonka et al., 2013). Hence, great attention has been drawn to glacial variation in this region. Field observations and monitoring have been conducted for several glaciers in this region. For example, in 1977–1978, a mountaineering expedition team conducted summer observations on Xiqiongtailan Glacier (a large scale valley glacier covering 164 km^2) in the southeast side of Mt. Tomor (Mountaineering and Expedition Term of Chinese Academy of Sciences, 1985). In this century, a number of observations have been conducted for the Koxkar Glacier on the south side of the Mt. Tomor since 2003 (a large scale valley glacier covering 83.56 km^2; this glacier and the Xiqiongtailan Glacier are both in the Tailanhe Basin; Xie et al., 2007; Han et al., 2008). However, the observations have been limited to a small area of the lower part and mainly on hydrology and meteorology, as well as changes in ice cliffs and supraglacial lakes in the debris-covered area because of this glacier's large scale and complex upper part morphology. From 2008, more studies have been conducted with respect to Qingbingtan Glacier No. 72 in the Kunma Like River Basin on the south side of Mt. Tomor, an avalanche-feeding cirque-valley glacier covering 5.23 km^2 with debris covered partially in lower part. In addition, sporadic observations have

The Cryosphere Discuss., doi:10.5194/tc-2016-138, 2016
Manuscript under review for journal The Cryosphere
Published: 18 July 2016

been taken for some other glaciers in the region. Some previous observations have been reported on the terminus and thickness change of Qingbingtan Glacier No. 72 (Wang et al., 2011, 2013).

In this paper, firstly we would comprehensively describe the glacial features of Qingbingtan Glacier No. 72 based on more observation data, and then the variation mechanism, response process to climate change and future scenarios were discussed for this glacier by analyzing the climatic and topographic factors.

2. Study site

The Tian Shan cover a large fraction of Central Asia and the Tomor region is in the inner ranges in Central Tien Shan (Fig. 1a). This region is heavily glaciated and glaciers contribute significantly to water supply in the arid lowlands. For example, glacial meltwater provides more than 50% runoff of the Aksu River (Yang et al., 1991; Kang et al., 2000), which is the largest tributary of Tarim River. In the source region of a branch of the Aksu River, named Kunma Like River, there is a glacier named Qingbingtan Glacier No. 72 (79°54' E; 41°45' N). It is located on the southern slope of Mt. Tomor, Tian Shan (Fig. 1a). According to the Glacier Inventory of China (Shi, 2005), it is a south-facing cirque-valley glacier (Fig. 1b and 1c). Based on a 1964 topographic map (1:50 000, based on aerial photographs), the glacier had an area of 7.27 km^2 and a length of 7.4 km. The elevations at the top and terminus are 5986 m and 3560 m, respectively, with an average elevation of 4200 m, and a snow line at 4300 m. According to a 2008 topographic map (1:50 000, from GPS measurement), the glacier area covered 5.74 km^2, with a length of 5.59 km, and a terminus elevation of 3720 m (Fig. 2 shows the variation of glacier terminus). The upper part of the glacier is composed of two cirques and a wide range of steep slopes. The glacier was mainly nourished from snow accumulation in the cirques and snow/ice avalanches from the steep slopes. The glacier tongue is long and narrow, with the debris covered in the western and eastern lateral sides. Glaciers in the Mt. Tomor region are commonly covered by debris and approximately 80% of the total number of glaciers in this

The Cryosphere Discuss., doi:10.5194/tc-2016-138, 2016
Manuscript under review for journal The Cryosphere
Published: 18 July 2016

region is debris covered to different extents (Shi, 2005). The Qingbingtan Glacier No. 72 can be considered as a representative of cirque-valley glacier partially covered with debris in the Mt. Tomor.

Mt. Tomor region was mainly influenced by westerlies from the Atlantic Ocean. The observation of two meteorological and hydrological stations shows that the average annual temperature of this region increased approximately at the rate of 0.44 ^{o}C (10a)$^{-1}$ and the annual precipitation increased by 2.99 mm (10a)$^{-1}$ since 1960 (will be mentioned in the section 5.2). With the atmospheric warming, glacier shrinkage and meltwater change in this region have reported both from remote-sensing studies (Bolch, 2007; Sorg et al., 2012; Pieczonka et al., 2013) and ground measurements (Zhang et al., 2006; Xie et al., 2007; Wang et al., 2011, 2013). For the Qingbingtan Glacier No.72, ground measurement started in 2008. The observation items include mass balance, ice velocity, terminus location, ice thickness, surface elevation, debris cover, meteorology and hydrology. In the following section, the observation procedure and data processing will be presented in detail.

The Cryosphere Discuss., doi:10.5194/tc-2016-138, 2016
Manuscript under review for journal The Cryosphere
Published: 18 July 2016

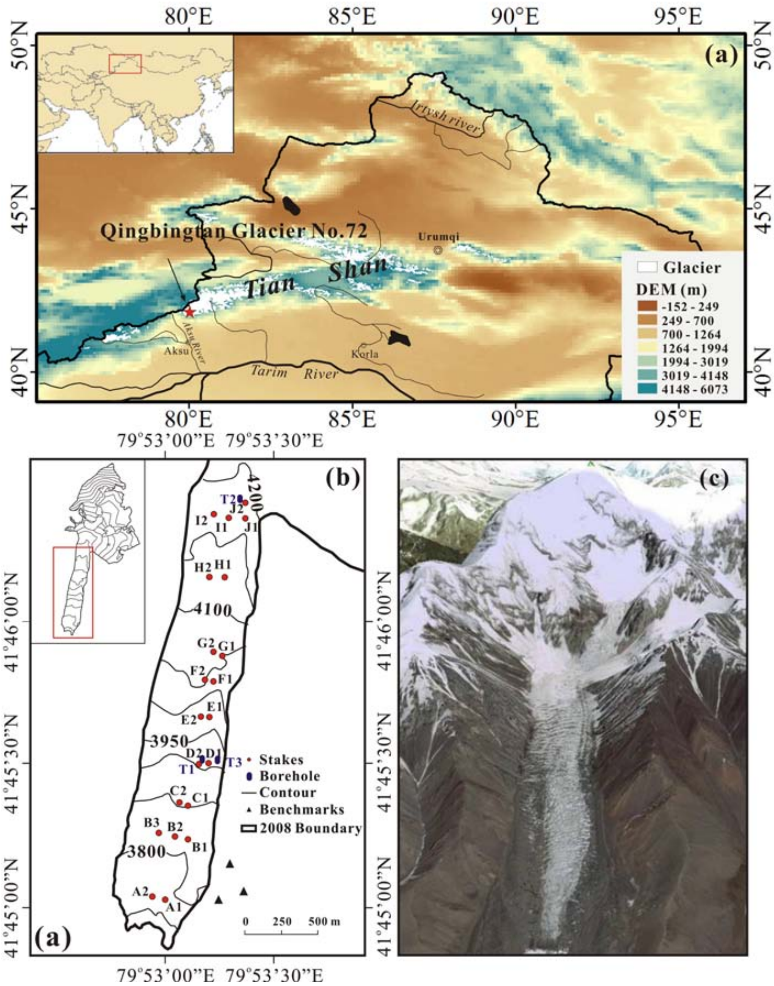

Figure 1. (a) The geographic location of Qingbingtan Glacier No. 72 in Mt. Tomor, Tian Shan, China; (b) Topographic map of Qingbingtan Glacier No. 72 and the surveyed area. Triangles are benchmarks for the GPS ground survey that are the national trigonometric reference points. Blue cylinders represent three ice temperature boreholes (T1 and T2: bare ice at 3950 m and 4200 m, respectively; T3: debris covered at 3950 m); (c) A satellite image of Qingbingtan Glacier No. 72 (data source: Google Earth).

3. Datasets and methods

3.1 Mass balance

Since the upper part of Qingbingtan Glacier No. 72 is steep, fragile and associated with frequent snow/ice avalanches (Fig. 1b and 1c), the mass balance field observations were only feasible below ~4200 m, i.e. in the glacial tongue zone (Fig. 1b), except for snow pits at 4400 and 4600 m. During the first investigation in 2008, totally 21 stakes were installed by a steam drill at 10 elevations of the tongue area (Fig. 1b). The mass balance measurement contains the vertical height of stakes over the glacier surface, thickness of affiliated ice, firn layer thickness and density, and structure of snow pits profiles at each stake. From the end of July to the beginning of September 2008, the stake mass balance measurement was carried out once almost every two days. In the following periods, the observation was conducted during the summer at least once a year.

The mass balance of a single point (b_n) can be obtained by

$$b_n = b_{ice} + b_s + b_{si} \quad (1)$$

where b_{ice}, b_s and b_{si} are the mass balance of glacier ice, snow and affiliated ice, respectively.

There are two commonly used methods to determine the specific mass balance of a glacier. One method is to interpolate from the measured data manually by drawing contour lines of equal mass balance (Paterson, 1994). The other method is to calculate from repeated measurements at ablation stakes at different altitudes. Although ten rows of 21 stakes were distributed in the glacier tongue area, they did not cover the entire ablation area completely. Therefore, the net ablation amount for the whole glacier could not be obtained directly from the observed results. The accumulation rate can be estimated roughly only from precipitation data and snow-pit observation. It is difficult to assess the accuracy of the glaciological mass balance because of

The Cryosphere Discuss., doi:10.5194/tc-2016-138, 2016
Manuscript under review for journal The Cryosphere
Published: 18 July 2016

various sources of uncertainty such as internal accumulation and ablation (Rabus and Echelmeyer, 1998), and calving (Arendt et al., 2002). According to Haeberli et al. (1998), generally the accuracy of the glaciological mass balance is in the centimeter to decimeter range.

3.2. RTK-GPS survey

3.2.1. Ice flow velocity

A real time kinematic global positioning system (RTK-GPS) (Unistrong E650) manufactured by Beijing UniStrong Science and Technology Co., Ltd. Beijing, China was used to measure the positions of the ablation stakes of Qingbingtan Glacier No. 72 starting in 2008. One GPS receiver was installed at a fixed base point on a non-glaciated area to the southeast of the glacier margin. Another was used to survey simultaneously the ablation stakes on the glacier. The displacement vectors could be obtained based on two measurements within a certain period, which were then taken as the ice flow velocity at each corresponding position. In this way, the ice flow velocity provided here was actually the surface velocity, and, therefore, could be decomposed into two components, horizontal and vertical velocities. The positions of 21 ablation stakes (Fig. 1b) in the tongue area of Qingbingtan Glacier No. 72 were measured in August 2008 and every summer in the following periods. Because the ablation stakes were rearranged after every measurement, the measurement result in 2008–2009 was used as an example. The GPS measuring in RTK differential mode results in a horizontal error of 0.02 m and a vertical error of 0.02–0.04 m, which is larger than the horizontal value. Accordingly, Errors in the computed velocity were within 8% of the input data.

3.2.2. Surface elevation

Furthermore, the surface elevation in and around the glacier tongue was measured at a sampling

The Cryosphere Discuss., doi:10.5194/tc-2016-138, 2016
Manuscript under review for journal The Cryosphere
Published: 18 July 2016

spacing of 20-50 m using RTK-GPS during the investigation in 2008, allowing the preparation of a large scale (1:50 000) topographic map. Accordingly, the ice surface elevation changes of glacier tongue can be obtained by comparing with 1964 topographic map (1: 50 000). First, the 1964 topographic map was digitized into a 5 m resolution digital elevation model (DEM). Then, the variations in ice surface elevation during the period from 1964 to 2008 could be derived. From 1964 topographic map and 2008 GPS data, ten discrete independent control points in the surrounding non-glaciated area were selected to perform the accuracy of ice surface elevation (σ_{DEM}) using the equation:

$$\sigma_{DEM} = \frac{\sum_{1}^{n}\left(Z_{DEM1964} - Z_{DEM2008}\right)}{n} \quad (2)$$

where n is the number of non-glacierized DEM grid cells. The results indicated that the error of surface elevation variations was within ± 6 m.

3.2.3. Glacier terminus and area changes

To determine glacier terminus and area changes, various data were obtained to make a comparison, including a topographic map in 1964 (1:50 000), a SPOT5 image (resolution: 5 m) in 2003, and the glacier terminus position measured by RTK-GPS during the investigation in 2008 and in summer of following years 2009, 2010, 2011, 2012 and 2013. All these data were put into the same coordinate system, which is an important precondition for precisely calculating changes in glacier terminus, area and surface elevation. Glacier boundaries for the different periods were digitized manually in the software ARCGIS. For the period 1964–2008, according to Williams et al. (1997), Hall et al. (2003), Silverio and Jaquet (2005), and Ye et al. (2006), the uncertainty in the glacier area and terminus changes for an individual glacier can be estimated by

$$U_T = \sqrt{\sum \lambda^2} + \sqrt{\sum \varepsilon^2} \quad (3)$$

$$U_A = \sum \lambda^2 \times \frac{2 \times U_T}{\sqrt{\sum \lambda^2}} + \sum \varepsilon^2 \quad (4)$$

where U_T is the uncertainty of the glacier terminus, λ is the resolution of each individual image, and ε is the registration error of each image to the 1964 topographic map. For the accuracy of glacier terminus and area changes during 2008–2013, it mainly depends on the GPS measuring error, although the error using a seven-parameter space transform model for transforming coordinate of GPS data that is less than 0.002 m (Wang et al., 2003), cannot be ignored. Integrated evaluation indicated that the resulting uncertainties of glacier terminus and area variation are 18 m and 0.012 km^2 in 1964–2008, and 0.24 m and 0.003 km^2 in 2008–2013, respectively.

3.3. Ice thickness

In August 2008 and July 2009, a pulse EKKO PRO 100A enhanced ground penetrating radar (GPR; Sensors & Software Inc., Mississauga, Canada) in combination with RTK-GPS was adopted to measure the glacier thickness. As shown in Fig. 3a, the ice thickness survey was conducted along five transverse and four longitudinal sections with a total of 824 measurement points. Since there is a crevasses area above 3950 m, the longitudinal cross section along the main flowline was divided into two segments (B–B and D–D). Horizontal survey was conducted along an east-west direction, while the longitudinal survey started from the high elevation. Surveyors were unable to extend some survey lines to the glacier margins because of its steep slopes. The spatial coordinates of survey points were recorded simultaneously, thereby achieving terrain correction for every survey point. The GPR data were then processed in the software EKKO_View Deluxe. The ice thickness (h) can be calculated by the equation (5), and the relative error of ice thickness measurement can be estimated by the equation (6) (Sun et al. (2003)):

$$h = \frac{t_s}{2} \times v \tag{5}$$

$$\frac{dh}{h} = \frac{dv}{2v} \tag{6}$$

where t_s is the radar wave two-way travel time and v is the velocity of radar signal in glacier. In this study, the velocity was set at 0.169 m $(ns)^{-1}$ after field trial for many times and the value is within the range of 0.167–0.171 m $(ns)^{-1}$ for the velocity of radar signal in mountain glaciers (Glen and Paren, 1975; Robin, 1975; Narod and Clarke, 1994). The estimation result indicated that the relative error of ice thickness measurement was within 1.2%. Ice thickness distribution map was eventually obtained by Kriging Interpolation Method assuming the thickness at the glacier margin to be zero.

3.4. Ice temperature and thickness of debris cover

At the end of July 2008, three ice temperature measurement boreholes were respectively drilled by a thermal steam drill in the bare ice at ~3950 m (T1; near to stake D2) and ~4200 m (T2), and in the debris covered area at ~3950 m (T3) (see Fig. 1b). The holes were 10 m deep in bare ice area and 2 m deep in debris covered area with the debris thickness of 13 cm. Thermistor temperature probes were buried at a depth interval of 0.5 m in bare ice area and 0.2 m in debris-cover. Ice temperature from the three boreholes (T1, T2, and T3) were measured respectively at the beginning of August 2008, and May, July, and September of 2009. The error of observed temperatures is within 0.1℃ according to similar works previously.

In August 2008, the thickness of debris cover is measured by digging the debris at the spacing of ~5 m on both lateral debris-covered areas of Qingbingtan Glacier No. 72. Moreover, six measuring ablation stakes were installed in debris-covered area to observe the melting difference

The Cryosphere Discuss., doi:10.5194/tc-2016-138, 2016
Manuscript under review for journal The Cryosphere
Published: 18 July 2016

under different thickness debris-covers.

In addition, an automatic weather station was set at ~3950 m during the investigation in 2008, and three more were installed at ~3800 m, ~3500 m and ~2800 m after 2009. A hydrologic section was placed ~2 km from the glacial terminus. Since theirshort observation period, the Aksu Meteorological Station (80°14′ E, 41°10′ N; 1104 m a.s.l.) and Xiehela Hydrologic Station (79°37′ E, 41°34′ N; 1487 m a.s.l.) were selected for long-term meteorological data analysis. These two stations are ~75 km southeast and ~30 km southwest to Qingbingtan Glacier No. 72, respectively. Because the Xiehela Hydrological Station has not been included in China's meteorology station network, only data before 2000 could be collected.

4. Results and analyses

4.1. Change in glacier terminus and area

From comparison of 1964 topographic map and 2008 RTK-GPS survey data, the elevation of the glacier terminus increased from 3560 m to 3720 m and the terminus position had retreated by 1811 ± 18 m at an average rate of 41.16 m a^{-1}. By comparing the SPOT5 remote sensing images of 2003 with on-site investigation in 2008, the recession was 240 ± 10 m or 48 m a^{-1} during the five years. The following field investigations show that the annual recession rates during 2008–2013 were 40.8 ± 0.05 m a^{-1}, 41 ± 0.06 m a^{-1}, 30 ± 0.05 m a^{-1}, 27 ± 0.04 m a^{-1}, and 22 ± 0.04 m a^{-1}, respectively. Thus, a general outline of the glacier terminus variations was obtained (Fig. 2). The glacier terminus has been retreating during the past 50 years and the most intensive retreat occurred at the end of 20th century and the beginning of this century. More recently, i.e. after 2009, the recession has slowed down because the debris cover enhanced the inhibition of glacier ablation, which will be discussed in detail below.

The Cryosphere Discuss., doi:10.5194/tc-2016-138, 2016
Manuscript under review for journal The Cryosphere
Published: 18 July 2016

In addition, by comparing various topographic maps, remote sensing image, and field survey data, the glacier tongue area had also shrunk beside recession of the terminus. The obtained glacier area shrinkage was 1.53 ± 0.012 km^2 at a rate of 0.034 km^2 a^{-1} between 1964 and 2008 and was 0.165 ± 0.005 km^2 or 0.033 km^2 a^{-1} between 2003 and 2008. The area declined by 0.124 ± 0.003 km^2 from 2008 to 2013 with a rate of 0.025 km^2 a^{-1}. The results indicated that the area reduction was large before 2008 and was alleviated afterwards, a similar trend to the terminus retreat. Table 1 compares the terminus and area variation between this glacier and other glaciers in the Mt. Tomor region. We can see that Qingbingtan Glacier No. 72 has the highest recession rate although its area is the smallest. The major potential reason for this is that the other glaciers are covered by debris completely in their lower parts and thus have smaller terminus recessions. Among those glaciers, the Koxkar Glacier had the best observation, which could represent the variation of glaciers with completely debris covered in a lower part (Xie et al., 2007). The Koxkar glacial terminus was basically stable before 1989, and then started to retreat. Since 2003, the recession was alleviated due to the enhanced inhibition of ablation by the debris-covered expansion.

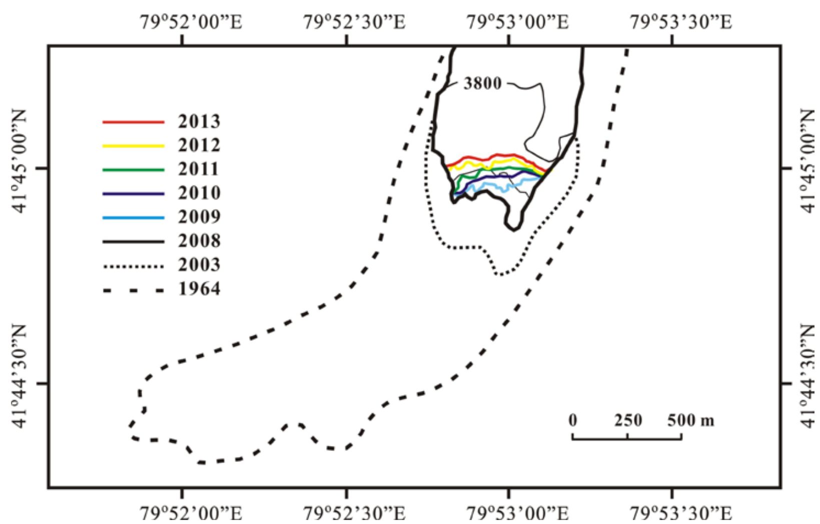

The Cryosphere Discuss., doi:10.5194/tc-2016-138, 2016
Manuscript under review for journal The Cryosphere
Published: 18 July 2016

The Cryosphere Discussions

Figure 2. Schematic graph of boundary changes of the tongue area of Qingbingtan Glacier No. 72.

Table 1 Comparison of the terminus and area variations between the Qingbingtan Glacier No. 72 and other glaciers in the Mt. Tomor region.

Glacier	Debris cover	Glacier area	Glacier length	Terminus change		Area change		Source
		km^2	Km	Period	$m\ a^{-1}$	Period	$km^2\ a^{-1}$	
Qingbingtan Glacier No. 72	Partially covered	7.27	7.4	1964–2008	−41.16	1964–2008	−0.034	This study
				2003–2008	−48.00	2003–2008	−0.033	
				2008–2013	−32.16	2008–2013	−0.025	
Keqikar Glacier	Completely covered in a lower part	83.6	26	1976–1981	0.0	—		Wang and Su, 1984
				1981–1985	−4.0	—		Zhu, 1982; Wang, 1987
				1985–1989	0 or 2	—		Xie et al., 2007
				1989–2003	−18–−20	—		Xie et al., 2007
				2003–2010	−11–−15	—		Han, Personal communication
Qingbingtan Glacier No. 74	Completely covered in a lower part	9.55	7.5	1964–2009	−30.0	1964–2009	−0.031	Wang et al., 2013
Keqikekuzibayi Glacier	Completely covered in a lower part	25.77	10.2	1964–2007	−22.9	1964–2007	−0.041	Wang et al., 2013
Tomor Glacier	Completely covered in a lower part	310.14	41.5	1964–2009	−3.0	1964–2009	−0.021	Wang et al., 2013
Qiongtailan Glacier	Completely covered in a lower part	164.38	23.8	1942–1976	−17.6	—		Su et al., 1985
				1964–2003	−22.0	1964–2003	−0.119	Wang et al., 2013

4.2. Changes in glacier thickness and surface elevation

As shown in Fig. 3b, the maximal ice thickness of the glacier tongue is 148 m, occurring in the

The Cryosphere Discuss., doi:10.5194/tc-2016-138, 2016
Manuscript under review for journal The Cryosphere
Published: 18 July 2016

upper part of the tongue close to the main flowline. The tongue area is generally thin and smooth, except for at the elevation of ~4200 m, where the thickness and its spatial variation are relatively large. Fig. 3c and 3d illustrate the glacier cross section from the a–a radar image profile and longitudinal section from B–B and D–D radar image profiles, respectively, which could reflect the basic characteristics of horizontal and longitudinal changes of the ice thickness and elevations of the glacier surface and the bedrock. From these figures it can be seen that the maximum thickness along the main flowline in longitudinal section occurs above ~4000 m a.s.l., and the thickness is larger in the central in the horizontal sections. Compared to the surface elevations, the bedrock exhibits large undulations, especially at ~4000 m a.s.l., where persistent undulations occur on the same level.

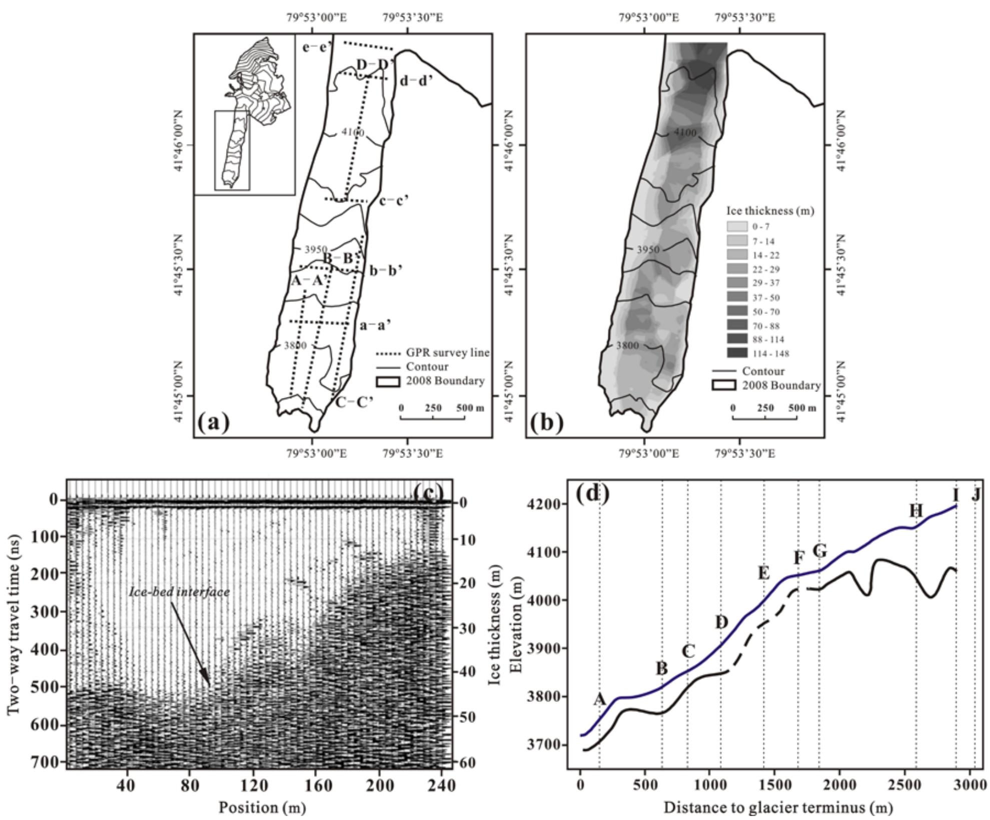

The Cryosphere Discuss., doi:10.5194/tc-2016-138, 2016
Manuscript under review for journal The Cryosphere
Published: 18 July 2016

Figure 3. (a) Ground penetrating radar survey sections of Qingbingtan Glacier No. 72; (b) Ice thickness distribution map of the glacier tongue; (c) An example of the radar image showing the cross section profile (a–a); (d) variations of the surface and the bedrock elevations along the main flowline (based on radar image section B–B and D–D).

Since lack of earlier thickness measurements, the temporal changes of the ice thickness could be obtained only from the variations in the surface elevation. The derived surface elevation variations are shown as Fig. 4. This result reveals that the ablation area of the glacier was generally in a thinning tendency. Between 1964 and 2008, the reduction in thickness was 9.59 ± 6 m, with an average reduction rate of 0.22 ± 0.14 m a^{-1}. A small area at ~4200 m exhibited a slight amount of thickening, which was probably caused by the net difference between upper stream feeding and ablation. Meanwhile, it was also found that the variation in the surface elevation in the central was more obvious than on the two lateral sides. This might be caused by debris covering on both sides. The influence of debris cover on glacial ablation will be discussed below.

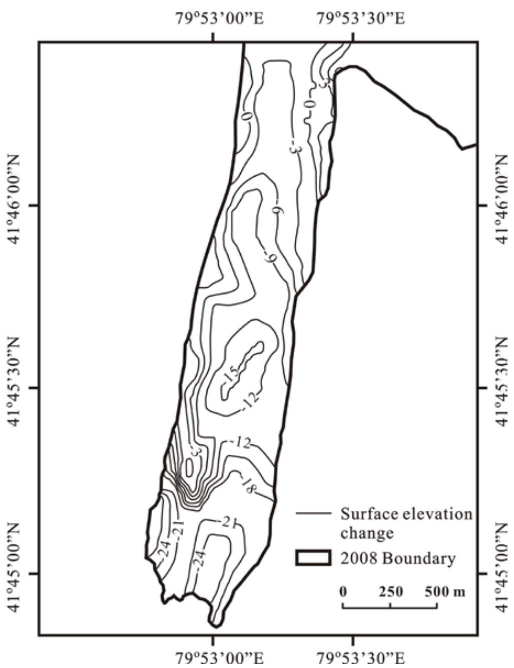

Figure 4. The isogram map of the surface elevation variations in the tongue area of Qingbingtan Glacier No. 72 during 1964–2008.

4.3. Changes in glacier mass and volume

As stated above, despite the small scale of Qingbingtan Glacier No. 72, it has complex morphology, making it difficult to conduct mass balance observation. Based on the limited observational data from August 2008 to August 2009, the lowest row of stakes (~3760 m) showed an annual net ablation of 6000−7000 mm, and the highest row demonstrated 1100 mm of annual ablation. Taking the average value of stakes in every row as the net ablation of the corresponding elevation, the variation of net annual ablation with elevation could be derived (Fig. 5). For areas below ~3820 m and above ~4020 m, there was a linear relationship between net annual ablation and elevation. However, the variation between ~3820 m and ~4020 m was irregular. From the topographic map (Fig. 1b) and on-site observations (Fig. 1c and Fig. 6), the

The Cryosphere Discuss., doi:10.5194/tc-2016-138, 2016
Manuscript under review for journal The Cryosphere
Published: 18 July 2016

surface was relatively flat without mount shelter influence between 3760 m and 3820 m a.s.l. so that the ablation was extremely strong near the terminus and decreased linearly with increasing elevation. Between ~3820 m and ~4020 m, the glacier surface was uneven and so the ablation was complex. Between ~3820 − ~3850 m, the surface is very rugged with undulations as high as 10−20 m, and there were surface streams as well as scattered debris composed of black and brown rock, which contributed to the tendency of increasing ablation with rising elevation. Between ~3850 − ~3930 m a.s.l., the surface became smooth again, showing similar ablation conditions as observed at the glacial terminus. Between ~3930 − ~4020 m, because of shielding and shades of high mountains on both sides, only a small area received direct sunlight. Meanwhile, the glacier surface undulations reached more than 20 m and surface lakes formed. The ablation amount increased slightly with increasing elevation. Above the elevation of ~4020 m, the glacier surface became smooth and even, and the ablation was weak and decreased with increasing elevation. In addition, high amounts of precipitation fell in the area above ~3950 m during the field observations, mainly in the form of sleet.

The Cryosphere Discuss., doi:10.5194/tc-2016-138, 2016
Manuscript under review for journal The Cryosphere
Published: 18 July 2016

332 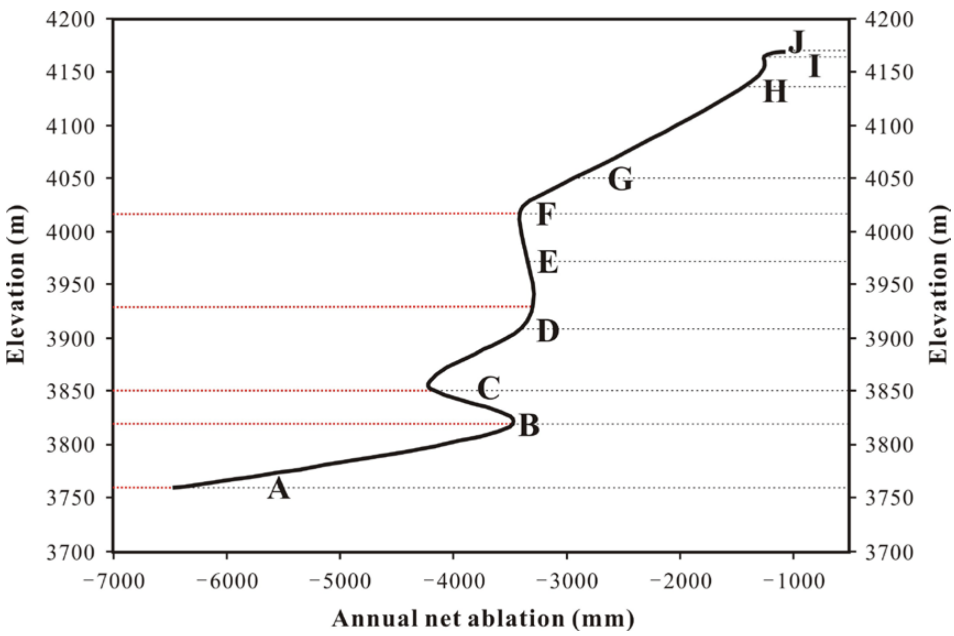

333 **Figure 5.** Variation of the annual net ablation along with elevation of Qingbingtan Glacier No.

334 72.

335

336 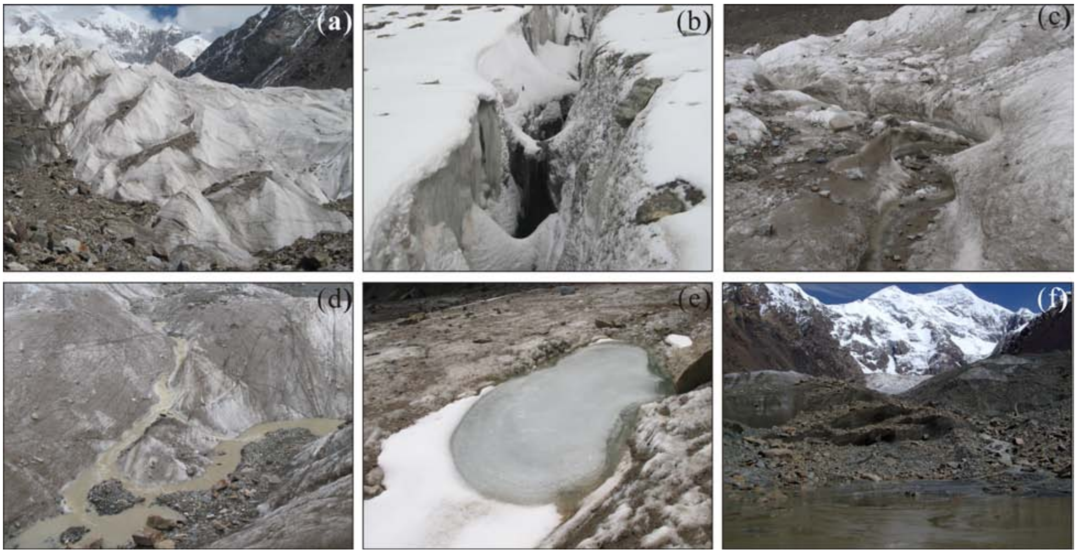

337 **Figure 6.** Photos showing the surface features of Qingbingtan Glacier No. 72.

Via extrapolation of the linear variation above ~4020 m, it could be roughly estimated that the equilibrium-line elevation (ELA) was at ~4250 m. However, the topographic map and satellite images showed that the terrain became steeper above ~4250 m, and the region was separated into three ice feeding areas. In the sun-facing eastern and middle feeding areas, ablation occurred even at ~4400 m; however, in the western area, mountain shade created an accumulation area above ~4200 m. Thus, it could be estimated that the equilibrium-line altitude was about 4300 m, and did not change significantly. This was true because the frequent avalanches and snow accumulation occurred in the upper part with steep slopes and small depressions. Therefore, the area of the ablation zone was 1.66 km^2 according to the 2008 map, with a net annual ablation of 3.93×10^6 m^3 and an average net annual ablation depth of 2367 mm. From meteorological observations in the ablation zone and the observation data from other glaciers in the same region, the annual precipitation in the glacial ablation area averaged about 700 mm. Thus, the total annual ablation was 5.09×10^6 m^3, and the average annual ablation depth was 3066 mm.

The complex terrain of the accumulation zone makes the net accumulation hard to estimate, even though observation of snow pits had been conducted in the eastern firn basin at ~4400 m and ~4600 m. According to data from the scientific expedition of Mt. Tomor in the 1970s (Xiqiongtailan Glacier observation results; Mountaineering and Expedition Term of Chinese Academy of Sciences, 1985), the annual precipitation at and above ~4200 m was over 800 mm, and the maximum precipitation of 1000 m was found at ~5200 m. Considering the increasing precipitation received in the Xinjiang Uygur Autonomous Region since the 1980s (as seen from the data of meteorological and hydrological stations shown below), the average annual precipitation in the accumulation area was not less than 1000 mm. Given no water loss in the accumulation area, the total annual accumulation could be 4.10 × 10^6 m^3. Hence, it could be derived that the annual net mass balance of the glacier was −990 × 10^3 m^3 and the specific annual net mass balance was −172 mm water depth.

Furthermore, the glacier mass balance over the past decades could be evaluated via the variation in glacier volume change, i.e. geodetic mass balance (Zemp et al., 2010). According to the variation of glacier thickness obtained in the part 4.2 mentioned above, the volume reduction between 1964 and 2008 caused by tongue area thinning (only the measured area of 1.47 km^2) was (14.1 ± 8.8) × 10^3 km^3, i.e. a water equivalent of (12.7 ± 7.9) × 10^3 km^3 if assuring ice density of 900 kg m^{-3}. Thus, the average annual mass loss was (288.6 ± 179.5) × 10^3 m^3, with the specific annual net mass balance of 50 ± 31.2 mm water depth. If extrapolating the thickness reduction to the entire ablation area, the number would be higher, but still smaller than the current net mass balance value. Although these estimates are very rough, the results suggest this glacier is currently in the stage experiencing lager mass loss.

4.4. Debris cover and its influence on glacier ablation

A number of previous studies have investigated the influence of the debris cover on glacier ablation (Han et al., 2010; Bolch et al., 2012; Pieczonka et al., 2013, 2015; Pellicciotti et al., 2015; Pratap et al., 2015). Glaciers in the Mt. Tomor region are commonly covered with debris and the debris cover was investigated on the Koxkar Glacier (Han et al, 2010). Generally, the debris-cover within a few centimeter of thickness is believed to promote glacier ablation, and the debris cover starts to inhibit ablation when its thickness reaches a certain value. The critical thickness is largely associated with debris size and rock properties. For example, the high porosity of coarse-grained material allows high rates of thermal transmission, as do substances with high thermal conductivity. Based on observation of six measuring points across the debris covered area at an elevation of ~3950 m in Qingbingtan Glacier No. 72, the critical thickness was about 4 cm, while it was 5 cm for the Koxkar Glacier (Han et al., 2010). Therefore, even glaciers in the same region behave apparently different. Moreover, the alleviation of ice melting will be higher with increasing thickness of debris cover after exceeding the critical thickness. Based on the observations of Qingbingtan Glacier No. 72 in August 2008, when the debris cover thickness exceeded 0.4–0.5 m, the ice melting beneath became negligible.

The debris covered area on the glacier was 0.87 km^2, in which the debris cover thicker than 4 cm was 0.66 km^2, accounting for 40% of the ablation area. Fig. 7 shows the thickness distribution of debris cover on the glacier. Overall, the debris cover on this glacier has an alleviating ablation effect. Because flaky and spotty debris were scattered over the bare ice area, their promotion for ablation was obvious; but no detailed observation on them. However, we could still speculate that with further ablation, the flaky and spotty debris will continuous accumulate to form a consecutive distribution gradually.. Meanwhile, the debris-covered area on both lateral sides will expand towards the main flowline. With further increase in debris cover thickness and area, some extent from the glacier terminus to upper part will be completely covered by debris finally, similar to the other glaciers mentioned above in the Mt. Tomor region. In this case, the total ablation would and hence the area shrinkage decrease markedly.

The Cryosphere Discuss., doi:10.5194/tc-2016-138, 2016
Manuscript under review for journal The Cryosphere
Published: 18 July 2016

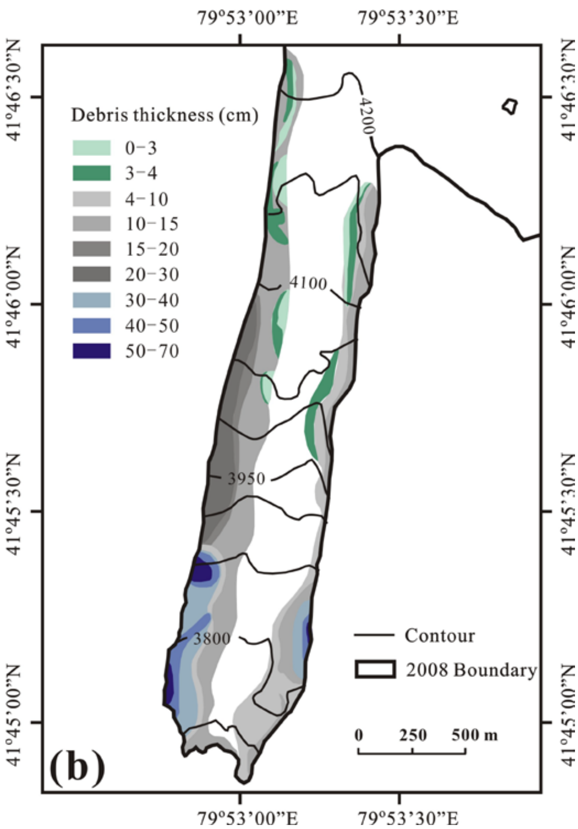

Figure 7. The thickness distribution of debris cover on Qingbingtan Glacier No. 72.

4.5. Ice flow velocity

Since the stakes at a same section were relatively near to each other, the velocity difference between adjacent stakes was small. The stake close to the main flowline moved faster than others in the same section. Fig. 8a shows the annual average horizontal velocity of every section between August 2008 and August 2009. The minimal horizontal speed, 18.6 m a^{-1}, appeared at the J cross section at an elevation of ~4170 m, where the surface slope was rather gentle, and the bedrock had large undulations around a roughly same elevation as well as ice thickness was relatively very large (see Fig. 3 for longitudinal profiles of ice thickness, elevation and slope).

The maximum speed, 70 m a^{-1}, was observed at the G cross section at an elevation of ~4050 m, where there was a turning point of changes in surface slope and ice thickness since slope increased and ice thickness decreased sharply downstream from this section. Below the elevation of ~3900 m, the surface slope gradually decreased, ice thickness had no change almost and the ice velocity decreased continuously. At the B cross section at an elevation of ~3820 m, the velocity decreased to 20 m a^{-1}. At the A cross section with the lowest elevation, the annual ablation depth was approximately 7 m. Because the stakes fell down, the velocity was only available for a short period. When compared with the B' cross section, the velocity at A' was slightly elevated, which corresponded to the increase of the terminus slope. The change in vertical velocity with elevation was similar to the horizontal velocity (Fig. 8b); the maximal value, 15 m a^{-1}, was present at the F cross section at an elevation of ~4016 m, which was a little lower than the G cross section where the maximal horizontal velocity occurred. From the results, one can conclude that surface slope was the main factor controlling the velocity distribution. Based on the results of all measuring points, the annual average horizontal velocity over the entire observed area was 47.61 m a^{-1}, which was higher than most cirque-valley glaciers observed in the Tian Shan (Jing et al., 2002, 2011; Zhou et al., 2009; Wang et al., 2016). This suggests that the basal sliding has an important contribution to the glacier movement.

Furthermore, Fig. 8 gives the comparison of the average monthly velocity in ablation season (June–August) with the average monthly velocity of every section. It can be seen that average monthly velocity was lower than that in the ablation season. By averaging the values of all points, the average monthly horizontal velocity was 3.95 m per month and 6.46 m per month in the ablation season, and the average monthly vertical velocity was 0.58 m per month and 1.54 m per month in the ablation season. The higher velocity during the ablation season should be attributed to the meltwater lubricating at the bedrock, which has an enhancing effect on the glacial sliding.

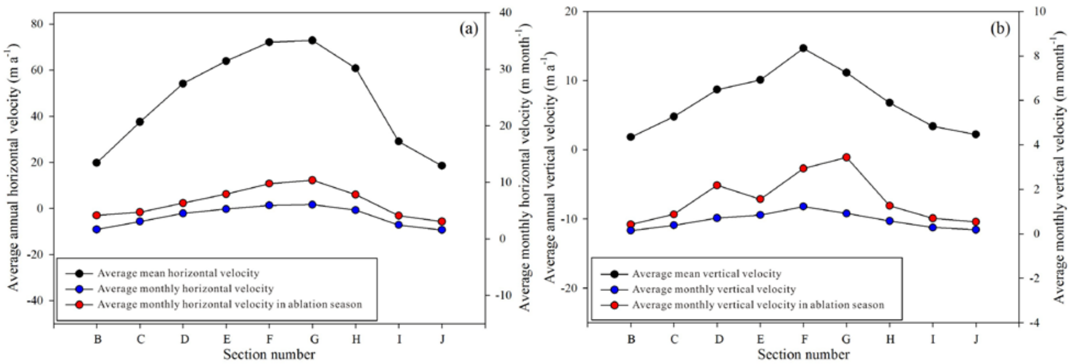

Figure 8. The surface velocity in the ablation area of Qingbingtan Glacier No. 72 between August 2008 and August 2009. (a) and (b) show the variation of horizontal and vertical velocity with elevation increasing, respectively.

4.6. Ice temperature

Ice temperature is an important index of the physical characteristics of a glacier. The measurement results in the boreholes drilled in the bare ice at the elevation of ~3950 m (T1) and ~4200 m (T2) show that the ice temperature within a depth of 10 m in the ablation area was higher than −2°C in summer and was −1.2 ℃ at 10-m depth. In the debris-covered area at the elevation of ~3950 m (T3), ice temperature within a depth of 2 m was higher than −1°C. Fig. 9 illustrates the temperature of three boreholes observed in the early August of 2008. Although no observations were conducted in winter, one can speculate that the temperature will drop below −2°C within only a few meters of depth. In the Mt. Tomor region, the annual precipitation is 600–800 m at elevations between 3700–4200 m, 40% of which fell during the non-ablation season (Han et al., 2008) and so the surface snow layer could be deeper than 1 m during winter. Thus, according to the simple model of heat conduction in the near surface layer of a glacier

The Cryosphere Discuss., doi:10.5194/tc-2016-138, 2016
Manuscript under review for journal The Cryosphere
Published: 18 July 2016

The Cryosphere Discussions Open Access EGU

(Paterson, 1994), the propagation depth of a cold wave in winter was within 5 m. Moreover, the heat released from refreezing of the meltwater stored in summer will offset the cold wave propagation. When the depth was greater than 10 m, the temperature would increase further. Therefore, temperature at the glacier bottom must be at the melting point, which benefits to the glacier sliding.

The condition in the accumulation area of this glacier was complex. At places with relatively smooth terrain, snowfall and avalanches contribute to high snow accumulation and percolation of meltwater in summer and refreezing in winter could profoundly increase the temperature of snow. At places with steep terrain, because snow layer is thin and thus the effect of meltwater percolation and refreezing is relatively weak, the temperature remained low. In general, the glacier temperature was high, in a way that is similar to the temperate or the monsoonal maritime glaciers.

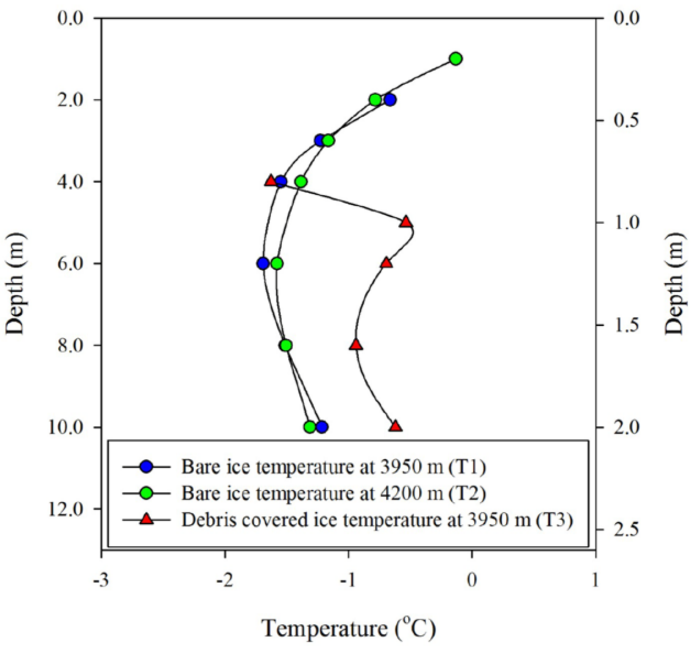

The Cryosphere Discuss., doi:10.5194/tc-2016-138, 2016
Manuscript under review for journal The Cryosphere
Published: 18 July 2016

Figure 9. The measured temperatures in 10 m-depth boreholes in the bare ice at ~3950 m (T1) and ~4200 m (T2), and in a 2 m-depth borehole with debris covered (T3) of Qingbingtan Glacier No. 72 in the early August 2008.

5. Discussion

5.1 Glacier behavior

Shape, size and physical properties of glaciers mainly depend on climatic and topographic conditions. In China, glaciers have commonly been classified the monsoon maritime and the continental types (Shi, 2005). The maritime glaciers exist in the southeastern Tibet Plateau under maritime climate and are believed to be characterized by high mass turnover (both accumulation and ablation are high) and ice temperature (major part of ice is at or near the melting temperature) and fast velocity due to broad basal sliding. The glaciers in other regions within China are usually regarded to be the continental type and their mass turnover, temperature and velocity are generally smaller apparently compared to the maritime type. However, these indexes have a large variability between various size and topographic glaciers in a same region and even within a same glacier, and so the ice temperature at a depth of 10–20 m is usually taken as a key indicator of glacial physical properties. From observations as shown above, the temperature at 10 m depth on the Qingbingtan Glacier No.72 is about –1.2℃, higher than that on other glaciers in the Tomor region. For example, the 10-m temperature observed on the Qiongtailai Glacier was between –4 and –2℃ (Wang et al, 1985). Its velocity is also high compared to most of similar scale glaciers in Tian Shan within China (Xie and Liu, 2010). So the Qingbingtan Glacier No. 72 behaves as the monsoon maritime glaciers in the southeastern Tibet Plateau. This suggests that individual glacier has specific behavior in a same region so that it is hard to classify all glaciers

The Cryosphere Discuss., doi:10.5194/tc-2016-138, 2016
Manuscript under review for journal The Cryosphere
Published: 18 July 2016

into one type in a region.

Although some differences in physical properties and topographic features are existed between Qingbingtan Glacier No.72 and others, the shrinkage trend is consistent for all glaciers in Tomor region. To a larger extent, as Tian Shan, many different investigations also revealed glacier shrinkage in past decades. Sorg et al. (2015) summarized the regional differences of glacier shrinkage between the inner and outer ranges as well as between different size glaciers in Tian Shan. They showed that glacier shrinkage is less severe in the continental inner ranges than in the more humid outer ranges and shrinkage is especially pronounced on small or fragmented glaciers. These imply that glacier variation trend is determined basically by climate change and the variation amplitude and response process are dependent on local climate conditions and glacier characteristics such as glacier size, topography and physical properties. The Qingbingtan Glacier No. 72 is small compared to some lager glaciers such as Qiontailan, Keqikar and Tomor glaciers listed in Table 1, but it larger than most glaciers in the Aksu River basin since the average area of all glaciers in the basin is 2.4 km^2. In the Tomor region, most glaciers have debris-covered area to some extent. The Qingbingtan Glacier No.72 is partially covered by debris in lower part. In view of these, its behavior and variation process revealed from observed results mentioned above could be regarded as typical indicators of glaciers in the Tomor region.

5.2. Response to climate change

As we all know, climate is the essential factor determining glacier variation. The combination of temperature and precipitation is most important for the glacier mass balance, which will consequently cause dimensional changes of a glacier. Many studies have investigated the relative importance of temperature and precipitation for glacier mass balance and they have demonstrated that the mass balance is more sensitive to temperature than to precipitation, although the quantative relation depends on regional climate and topographic conditions (Oerlemans and Reichert, 2000; Bolch et al., 2012; Carturan et al., 2012; Yu et al., 2013; Baral et al., 2014). Some studies on glaciers in the Tian Shan also proved the dominant role of temperature for changes in mass balance (Duethmann et al., 2015). As shown in Fig. 10, the records of both stations revealed that the temperature in the region has tended to increase during the last several decades. The Aksu Meteorological Station has also recorded an obvious increasing trend for precipitation, while the increasing trend was weak at the Xiehela Hydrological Station. However, the inter-annual variability was larger at Xiehela Hydrological Station than that at the Aksu Meteorological Station. Although precipitation is generally much different between high mountains and low elevations, the overall long-term trend should be similar. In view of the significant recession of this and other glaciers in the Tomor region during the last decades (Xie et al., 2007; Wang et al., 2013), one can conclude that temperature increase played a decisive function, and precipitation increase was insufficient to offset the effects of increasing temperatures. According to regional meteorological estimates (Qin, 2012), the temperature in the Tian Shan is expected to continue increasing in the next decade or more. It is not certain if precipitation will continue to increase, despite of the large inter-annual variability. At least, possibility of continuous large increase in precipitation is less. Hence, considering the influence of climate change, the glacier will keep a tendency of net mass loss during the next decade, and the corresponding glacier terminus recession is expected to last much longer. Based on the simplest model of glacier response to the mass balance disturbance caused by climate change (Paterson, 1994), this type of small size valley glacier would be expected to experience a delay of several years and a response time of several decades. For this glacier, if taking the average thickness of 70 m in the ablation area, the ablation rate of 5~7 m a^{-1} at the terminus, the

The Cryosphere Discuss., doi:10.5194/tc-2016-138, 2016
Manuscript under review for journal The Cryosphere
Published: 18 July 2016

estimated response time is about 15 to 21 years. Since ablation rate may decrease with expending debris-covered area and ice thickness would be larger in the upper part of this glacier, the response time should be longer than 20 year. This implies that, even without climatic warming, the terminus recession caused by historic climate change will last for more than 20 years.

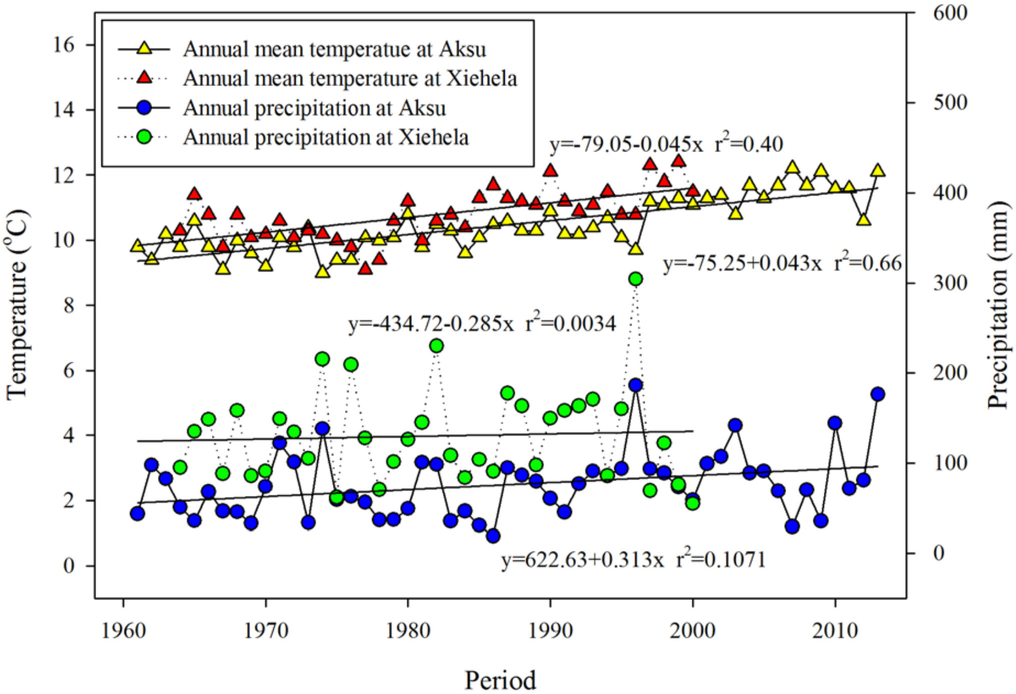

Figure 10. The temperature and precipitation variations recorded at Xiehela Hydrological Station and Aksu Meteorological Station since 1960.

5.3. Influences of topographic factors and debris cover

As mentioned above, Qingbingtan Glacier No. 72 has an irregular accumulation zone, and debris-covered parts in the ablation zone, both of which will greatly affect the glacier variation. In terms of the topographic factors, extremely steep slopes occur in the northern part in a wide range from ~4300 m up to about ~6000 m at the peak and snow/ice avalanches happen frequently.

The snow fall at high elevations could be rapidly transferred to the lower elevations. The two firn basins in the east were mostly below the elevation of ~5000 m and are the major snow accumulation area. The size of the accumulation area was generally stable.

The ablation area seems a regular rectangle on the plane and the debris-covered belts on both edges were generally thicker than the critical value required for the inhibition of ablation. Therefore, in the background of atmospheric warming, the bare ice area is expected to experience enhanced ablation and continuously thinning, and the debris-cover thickness and area will further increase. Because the bare ice area is narrow at the elevation ~4000 m, the debris-covered belts may be merged firstly at this elevation and then in the downstream area. Thus, ablation will be significantly reduced in the area below the elevation of ~4000 m and the recession of the terminus will become very small so that the glacier area will tend to remain stable and decrease in ice thickness will be the major characteristics. If the drastic atmospheric warming occurs, the ablation in the bare ice area will become surprisingly elevated. Perhaps the terminus will retreat to the elevation of 4000 m before the debris-covered belts is emerged. Because the accumulation area remains stable and the ice thickness above ~4100 m is very large, the glacier terminus is expected to remain at ~4100 m for a long period. One more possibility was that, with the debris-belts closing up in the lower area, the amount of ablation could decrease significantly, while ablation in the upper area increases continuously. The glacier may break and forms the new glacial terminus at the elevation of ~4000 m, and the lower part would then become a debris-covered independent area with slow movement and ablation. In summary, no matter which conditions occur, the glacier terminus is expected to retreat and stabilize at an elevation between ~4000 and ~4100 m in future decades.

The Cryosphere Discuss., doi:10.5194/tc-2016-138, 2016
Manuscript under review for journal The Cryosphere
Published: 18 July 2016

6. Conclusions

Qingbingtan Glacier No. 72 in Mt. Tomor region is a small size cirque-valley glacier with complex topography and debris-covered areas. In the accumulation zone, high precipitation and frequent avalanches provide plentiful mass supply, and in the ablation zone, melting is intensive with the annual net ablation of 7000 mm water depth near the terminus. The glacier temperature and movement are similar to the temperate or the monsoonal maritime glaciers of the southeastern Tibetan Plateau. From 1964 to 2008, the glacier had been in a continuous shrinkage, with the terminus retreat at 41 m a^{-1} and the area reduction of 1.53 km^2. Ice thickness in the ablation area decreased by 9.6 m on average during that time period. Despite persistent atmospheric warming, the strongest ablation and the most significant terminus recession and area reduction of the glacier occurred at the end of the last century and the beginning of this century rather than recent years because of an increasing inhibition of debris cover for ablation.

Atmospheric warming will cause further increase in ablation, but debris covered area will expand with melting enhance, which will inhibit surface melting. So the glacier is expected to keep shrinkage in the coming decades, but the terminus retreat is expected to be slower and slower, which has been proven by field observations since 2009. It may have occurred that the area below an elevation of ~4000 m became a fully debris-covered area, and then the terminus position was relatively stable. Furthermore, an intensive ablation increase in the upper bare ice area would have caused the lower debris covered area to break away from the upper part, resulting in sudden change of terminus position. From the surface and bed topography as well as data related to the distribution of ice thickness, the glacier is expected to remain stable over the long term after the terminus receded to the elevation of ~4000 m and the mass loss will be dominated by a reduction in ice thickness.

Further investigation and prediction of the glacier change should focus on gaining a substantial understanding of the dynamic processes, data acquisition from the upper stream and especially obtaining accurate results of mass balance in the time series.

Acknowledgments This research was funded by the Funds for Creative Research Groups of China (41421061), the Major National Science Research Program (973 Program) (2013CBA01801), the National Natural Science Foundation of China (41301069), the SKLCS founding (SKLCS-ZZ-2012-01-01), the West Light Program for Talent Cultivation of Chinese Academy of Sciences, and the Special Financial Grant from the China Postdoctoral Science Foundation (2014T70948).

References

Arendt, A.A. and 77 others: Randolph Glacier Inventory [v2.0]: A Dataset of Global Glacier Outlines. Global Land Ice Measurements from Space, Boulder, CO http://www.glims.org/RGI/randolph.html, 2012.

Arendt, A.A., Echelmeyer, K.A., Harrison, W.D., Lingle, C.S., and Valentine, V.B.: Rapid wastage of Alaska glaciers and their contribution to rising sea level, Science, 297 (5580), 382–386, 2002.

Baral, P., Kayastha, R.B., Immerzeel, W.W., Pradhananga, N.S., Bhattarai, B.C., Shahi, S., Galos, S., Springer, C., Joshi, S.P., and Mool, P.K.: Preliminary results of mass-balance observations of Yala Glacier and analysis of temperature and precipitation gradients in Langtang Valley, Nepal, Annals of Glaciology, 55(66), 9–14, 2014.

Berthier, E., Schiefer, E., Clarke, G.K.C., Menounos, B., and Rémy, F.: Contribution of Alaskan glaciers to sea-level rise derived from satellite imagery, Nature Geosci., 3(2), 92–95, 2010.

Bliss, A., Hock, R., and Radić, V.: Global response of glacier runoff to twenty-first century climate change, J. Geophys. Res.: Earth Surf., 119(4), 717–730, 2014.

Bolch, T. and 10 others: The state and fate of Himalayan glaciers, Science, 336(6079), 310–314, 2012.

Bolch, T.: Climate change and glacier retreat in northern Tien Shan (Kazakhstan/Kyrgyzstan) using remote sensing data, Global and Planetary Change, 56, 1–12, 2007.

Bolch, T., Pieczonka, T, Benn, D.I.: Multi-decadal mass loss of glaciers in the Everest area (Nepal Himalaya) derived from stereo imagery, The Cryosphere, 5, 349–358, 2011.

Carturan, L., Cazorzi, F., and Fontana, G.D.: Distributed mass-balance modeling on two neighbouring glaciers in Ortles-Cevedale, Italy, from 2004 to 2009, Journal of Glaciology, 58(209), 467–486, 2012.

Chen, Y.N., Xu, C.C., Hao, X.M., Li, W.H, Chen, Y.P, and Zhu, C.G.: Fifty-year climate change and its effect on annual runoff in the Tarim River Basin, China, Journal of Glaciology and Geocryology, 30(6), 921–929, 2008.

Duethmann, D., Bolch, T., Farinotti, D., Kriegel, D., Vorogushyn, S., Merz, B., Pieczonka, T., Jiang, T., Su, B., and Güntner, A.: Attribution of streamflow trends in snow and glacier melt-dominated catchments of the Tarim River, Central Asia, Water Resour. Res., 51, 4727–4750, 2015.

Farinotti, D., Longuevergne, L., Moholdt, G., Duethmann, D., Mölg, T., Bolch, T., Vorogushyn, S., and Güntner, A.: Substantial glacier mass loss in the Tien Shan over the past 50 years, Nature Geoscience, DOI: 10.1038/NGEO2513, 2015.

Fischer, M., Huss, M., and Hoelzle, M.: Surface elevation and mass changes of all Swiss glaciers

1980–2010, Cryosphere Discuss., 8(4), 4581–4617, 2014.

Glen, J.W., and Paren, J.G.: The electrical properties of snow and ice, J. Glaciol., 15, 15–38, 1975.

Haeberli, W., Cihlar, J., and Barry, R.G.: Glacier monitoring within the Global Climate Observing System, Ann. Glaciol., 31, 241–246, 2000.

Haeberli, W., Hoelzle, M., and Suter, S.: Into the second century of world glacier monitoring—prospects and strategies, UNESCO Publishing, Paris, 1998.

Haeberli, W., Paul, F., and Maisch, M.: Mountain glaciers in global climate-related observation networks, World Meteorological Organization Bulletin, Geneva, 51(1), 1–8, 2002.

Hall, D.K, Bayr, K., Schfner, W., et al.: Consideration of the errors inherent in mapping historical glacier positions in Austria from ground and space (1893–2001). Remote Sensing of Environment, 86, 566–577, 2003.

Han, H.D. and 13 others: Near-surface meteorological characteristics on the Koxkar Baxi Glacier, Tianshan, Journal of Glaciology and Geocryology, 30(6), 967–975, 2008.

Han, H.D., Wang, J., Wei, J.F., and Liu, S.Y.: Backwasting rate on debris covered Koxkar glacier, Tuomuer mountain, China, J. Glaciol., 56(196), 287–296, 2010.

Huss, M.: Extrapolating glacier mass balance to the mountainrange scale: the European Alps 1900–2100, Cryosphere, 6(4), 713–727, 2012.

IPCC: Working Group Ⅰ contribution to the IPCC Fifth Assessment Report (AR5), Climate Change 2013: The physical Science Basis, 2013.

Jing, Z.F., Liu, L., Zhou, Z.M. and Deng, Y.F.: Analysis on the influencing factors of glacier flow velocity: a case study of Qiyi Glacier in Qilian Mountains, Journal of Glaciology and Geocryology, 33(6), 1222–1228, 2011.

Jing, Z.F., Ye, B.S, Jiao, K.Q., Yang, H.A.: Surface velocity on Glacier No. 51 at Haxilegen of the Kuytun River, Tianshan Mountains, Journal of Glaciology and Geocryology, 24(5), 563–566, 2002.

Kang, E.S., Yang, Z.N., Lai, Z.M. et al.: Runoff of snow and ice meltwater and mountainous rivers. In: Shi Yafeng. Glaciers and their environments in China—The present, past and future. Science Press, Beijing, 2000.

Kehrwald, N.M., Thompson, L.G., Yao, T.D., Thompson, E.M., Schotterer, U., Alfimov, V., Beer, J., Eikenberg, J., and Davis, M.E.: Mass loss on Himalayan glacier endangers water resources, Geophys. Res. Lett., 35, DOI: 10.1029/2008GL035556, 2008.

Kutuzov, S., and Shahgedanova, M.: Glacier retreat and climatic variability in the eastern Terskey-Alatoo, inner Tien Shan between the middle of the 19th century and beginning of the 21st century, Global and Planetary Change, 69, 59–70, 2009.

Li, Z.Q., Li, K.M., and Wang, L.: Study on recent glacier changes and their impact on water resources in Xinjiang, North Western China, Quaternary Sciences, 30(1), 96–106, 2010.

Marzeion, B., Jarosch, A.H., and Hofer, M.: Past and future sealevel change from the surface mass balance of glaciers, The Cryosphere, 6(6), 1295–1322, 2012.

Meier, M.F., Dyurgerov, M.B., Rick, U.K., O’Neel, S., Pfeffer, W.T., Anderson, R.S., Anderson, S.P., and Glazovsky, A.F.: Glacier dominate eustatic sea-level rise in the 21st century, Science, 317(5841), 1064–1067, 2007.

Mihalcea, C., Mayer, C., Diolaiuti, G., Lambrecht, A., Smiraglia, C., and Tartari, G.: Ice ablation and meteorological conditions on the debris-covered area of Baltoro glacier, Karakoram, Pakistan, Ann. Glaciol., 43, 292–300, 2006.

Mountaineering and Expedition Term of Chinese Academy of Sciences: Glacial and Weather in

The Cryosphere Discuss., doi:10.5194/tc-2016-138, 2016
Manuscript under review for journal The Cryosphere
Published: 18 July 2016

Mt. Tuomuer District, Tianshan, Xinjiang Peoples Publishing House, Urumqi, 1985.

Narama, C., Kääb, A., Duishonakunov, M., Abdrakhmatov, K.: Spatial variability of recent glacier area changes in the Tien Shan Mountains, central Asia, using Corona (~1970), Landsat (~2000), and ALOS (~2007) satellite data, Global and Planetary Change, 71(1), 42–54, 2010.

Narod, B.B., and Clarke, G.K.C.: Miniature high-power impulse transmitter for radio-echo sounding, J. Glaciol., 40, 190–194, 1994.

Neckel, N., Kropácek, J., Bolch, T., and Hochschild, V.: Glacier mass changes on the Tibetan Plateau 2003–2009 derived from ICESat laser altimetry measurements, Environ. Res. Lett., 9(1), 014009, 2014.

Oerlemans, J.: Extracting a climate signal from 169 glacier records, Science, 308, 675–677, 2005.

Oerlemans, J. and Reichert, B.K.: Relating glacier mass balance to meteorological data by using a seasonal sensitivity characteristic, J. Glaciol., 46(152): 1–6, 2000.

Paterson, W.S.B.: The physics of glaciers, 3rd edn, Elsevier, Oxford, 1994.

Pellicciotti, F., Stephan, C., Miles, E., Herreid, S., Immerzeel, W.W., Bolch, T.: Mass-balance changes of the debris-covered glaciers in the Langtang Himal, Nepal, from 1974 to 1999, Journal of Glaciology, 61(226), 373–386, 2015.

Pieczonka, T., and Bolch, T.: Region-wide glacier mass budgets and area changes for the Central Tien Shan between ~ 1975 and 1999 using Hexagon KH-9 imagery, Global and Planetary Change, 128, 1–13, 2015.

Pieczonka, T., Bolch, T., Wei, J.F., and Liu, S.Y.: Heterogeneous mass loss of glaciers in the Aksu-Tarim Catchment (Central Tien Shan) revealed by 1976 KH-9 Hexagon and 2009

The Cryosphere Discuss., doi:10.5194/tc-2016-138, 2016
Manuscript under review for journal The Cryosphere
Published: 18 July 2016

SPOT-5 stereo imagery, Remote Sensing of Environment, 130, 233–244, 2013.

Pratap, B., Dobhal, D.P., Mehta, M., and Bhambri, R.: Influence of debris cover and altitude on glacier surface melting: a case study on Dokriani Glacier, central Himalaya, India, Annals of Glaciolgy, 56(70), 9–16, 2015.

Qin, D.H.: Climate and environment changes in China, vol 1, Meteorology Press, Beijing, 2012.

Robin G. de. Q.: Velocity of radio waves in ice by means of a bore-hole interferometric technique, J. Glaciol., 15, 151–159, 1975.

Rabus, B.T., Echelmeyer, K.A.: The mass balance of McCall Glacier, Brooks Range, Alaska, U.S.A.: its regional relevance and implications for climate change in the Arctic, J. Glaciol., 44(147), 333–351, 1998.

Raper, S.C.B. and Braithwaite, R.J.: Low sea level rise projections from mountain glaciers and icecaps under global warming, Nature, 439, 311–313, 2006.

Shi, Y.F.: Brief of Glacier Inventory of China, Shanghai Popular Science Press, Shanghai, 2005.

Silverio, W. and Jaquet, J.M.: Glacial cover mapping (1987–1996) of the Cordillera Blanca (Peru) using satellite imagery, Remote Sens. Environ., 95(3), 342–350, 2005.

Sorg, A., Bolch, T., Stoffel, M., Solomina, O., and Beniston, M.: Climate change impacts on glaciers and runoff in Tien Shan (Central Asia), Nature Climate Change, 2012. Doi: 10.1038/nclimate1592.

Su, Z., Sun, G.P., Wang, L.L., Zhang, W.J., Zhang, H.Y, Yang, C.T, and Liang, D.: Modern glacier in Mt. Tuomuer district. In: Su, Z., Kang, E.S. (Eds.), Glacial and Weather in Mt. Tuomuer District, Tianshan, Xinjiang Peoples Publishing House, Urumqi, 32–88, 1985.

Sun, B., He, M. B., Zhang, P., Jiao, K.Q., Wen, J. H., and Li, Y. S.: Determination of ice thickness, subice topography and ice volume at Glacier No. 1 in the Tianshan, China, by ground penetrating radar, Chinese Journal of Polar Research, 15(1), 35–44, 2003.

Wang, J.X., Wang, J., and Lu, C.P.: Problem of coordinate transformation between WGS-84 and BEIJING 54, J. Geod. Geodyn., 23(3), 70–73, 2003.

Wang, L.L., Zhang, W.J., and Song, G.P.: Glacier temperature. In: Glaciers and meteorology in Tomor region, Urumqi, Xinjiang People's Press, 64–69, 1985.

Wang, P.Y., Li, Z.Q., Wang, W.B., Li, H.L., Zhou, P., and Jin, S.: Changes of six selected glaciers in the Tomor region, Tian Shan, Central Asia, over the past ~50 years, using high-resolution remote sensing images and field surveying, Quaternary International, 311, 123–131, 2013.

Wang, P.Y., Li, Z.Q., Li, H.L., Wang, W.B., and Wang, F.T.: Ice surface-elevation change and velocity of Qingbingtan glacier No.72 in the Tomor region, Tianshan Mountains, central Asia, Journal of Mountain Science, 8, 855–864, 2011.

Wang, P.Y., Li, Z.Q., Li, H.L., Wang, W.B., Wu, L.H., Zhang, H., Huai, B.J., Wang, L.: Recent evolution in extent, thickness and velocity of Haxilegen Glacier No. 51, Kuytun River Basin, eastern Tianshan Mountains, Arctic Antarctic and Alpine Research, 48(2), 241–252, 2016.

Wang, S., Zhang, M., Li, Z., Wang, F., Li, H., Li, Y., Huang, X.: Glacier area variation and climate change in the Chinese Tian shan Mountains since 1960, Journal of Geographical Sciences, 21(2), 263–273, 2011.

Wang, Z.T.: Influence of supraglacial moraine on surface ablation and ice temperature of glaciers. In: The Lanzhou Institute of Glaciology and Geocryology, CAS. Proceedings of the 2nd National Conference on Glaciology of the Geographical Society of China, The People's Publishing House of Gansu, Lanzhou, 131–139, 1987.

Wang, Z.T., Su, Z.: A road on the glacier, Journal of Glaciology and Geocryology, 6(3), 95–96, 1984.

The Cryosphere Discuss., doi:10.5194/tc-2016-138, 2016
Manuscript under review for journal The Cryosphere
Published: 18 July 2016

World Glacier Monitoring Service (WGMS): Global glacier changes: facts and figures. UNEP, World Glacier Monitoring Service, Zürich http://www.grid.unep.ch/glaciers/, 2008a.

WGMS: Fluctuations of glaciers 2000–2005 (Vol. IX). ICSU (FAGS)/IUGG–(IACS)/UNEP/UNESCO/WMO, World Glacier Monitoring Service, Zürich (doi: 10.5904/wgms-fog-2008-12), 2008b.

WGMS: Fluctuations of glaciers 2005–2010 (Vol. X). ICSU(WDS)/IUGG(IACS)/UNEP/UNESCO/WMO, World Glacier Monitoring Service, Zürich (doi: 10.5904/wgms-fog-2012-11), 2012.

WGMS: Glacier Mass Balance Bulletin No. 12 (2010–2011). ICSU(WDS)/IUGG(IACS)/UNEP/UNESCO/WMO, World Glacier Monitoring Service, Zürich (doi: 10.5904/wgms-fog-2013-11), 2013.

Williams, R.S., Hall, Jr, D.K., and Chien, J.Y.L.: Comparison of satellite-derived with ground-based measurements of the fluctuations of the margins of Vatnajökull, Iceland, 1973–92, Ann. Glaciol., 24, 72–80, 1997.

Xie, C.W., Ding, Y.J., Chen, C.P., and Han, T.D.: Study on the change of Keqikaer Glacier during the last 30 years, Mt. Tuomuer, Western China, Environ. Geol., 51, 1165–1170, 2007.

Xie, Z.C., and Liu, C.H.: Introduction of Glaciology. Shanghai, Shanghai Science Popularization Press, 234–301, 2010.

Yang, Z.N.: Glacier water resources in China, Gansu Science and Technology Press, Lanzhou, 1991.

Yao, T., Thompson, L., Yang, W., Yu, W.S., Gao, Y., Guo, X.J., Yang, X.X., Duan, K.Q., Zhao, H.B., Xu, B.Q., Pu, J.C., Lu, A.X., Xiang, Y., Kattel, D.B., and Joswiak, D.: Different glacier status with atmospheric circulations in Tibetan Plateau and surroundings, Nature

The Cryosphere Discuss., doi:10.5194/tc-2016-138, 2016
Manuscript under review for journal The Cryosphere
Published: 18 July 2016

Climate Change, DOI: 10.1038/NCLIMATE1580, 2012.

Ye, Q.H., Kang, S.C., Chen, F., et al.: Monitoring glacier variation on Geladandong mountain, central Tibetan Plateau, from 1969 to 2002 using remote sensing and GIS technologies, Journal of Glaciology, 52(179), 537–545, 2006.

Yu, W.S., Yao, T.D., Kang, S.C., Pu, J.C., Yang, W., Gao, T.G., Zhao, H.B., Zhou, H., Li, S.H., Wang, W.C., Ma, L.L.: Different region climate regimes and topography affect the changes in area and mass balance of glaciers on the north and south slopes of the same glacierized massif (the West Nyainqentanglha Rang, Tibetan Plateau), Journal of Hydrology, 495, 64–73, 2013.

Zemp, M., Jansson, P., Holmlund, P., Gärtner-Roer, I., Koblet, T., Thee, P., Haeberli, W.: Reanalysis of multi-temporal aerial images of Storglaciären, Sweden (1959-99)–Part 2: Comparison of glaciological and volumetric mass balances, The Cryosphere, 4, 345–357, 2010.

Zemp, M., and 38 others: Historically unprecedented global glacier decline in early 21st century, Journal of Glaciology, 61(228), 745–762, 2015.

Zhang, Y., Liu, S., Ding, Y., Li, J., and Shangguan, D.: Preliminary study of mass balance on the Keqicar Baxi Glacier on the south slopes of Tianshan mountains, J. Glac. Geocry., 28, 477–484, 2006.

Zhou, Z.M., Li, Z.Q., Li, H.L., and Jing, Z.F.: The flow velocity features and dynamic simulation of the Glacier No. 1 at the headwaters of Urumqi River, Tianshan Mountains, Journal of Glaciology and Geocryology, 31(1), 55–61, 2009.

Zhu, G.C.: Type B-1 experimental radar instation for measuring the thickness of glaciers, Journal of Glaciology and Geocryology, 4(2), 93–95, 1982.